11th Australasian Fluid Mechanics Conference
University of Tasmania, Hobart, Australia
14-18 December 1992

EXPERIMENTAL STUDIES OF THE UNSTEADY VORTEX DYNAMICS OF A TWO-DIMENSIONAL PITCHING AIRFOIL

R.C. CONGER, H. OSHIMA and B.R. RAMAPRIAN

Mechanical and Materials Engineering Department
Washington State University
Pullman, WA 99164-2920, USA

ABSTRACT

Results of phase-locked surface pressure, velocity and vorticity measurements on an airfoil pitching at a constant angular velocity are presented. The experiments were performed in a free-surface water channel, using the technique of particle image velocimetry for the measurement of the instantaneous velocity field. These comprehensive data on pressure and vorticity are useful in understanding the unsteady vortex dynamics leading to the occurrence of dynamic stall on the pitching airfoil.

INTRODUCTION

The unsteady flow field around an airfoil undergoing a pitch-up maneuver in a steady stream has been studied with interest in recent years. This is because of the relevance of this study to practical applications such as super maneuverability of combat aircraft and aerodynamics of helicopter rotor blades. Experiments have shown that a much higher lift is generated by a pitching airfoil compared to a stationary airfoil and that stall is delayed until angles of attack much higher than in a steady flow field. These effects have been observed to occur in conjunction with the formation of large-scale vortical structures primarily near the leading edge on the suction side of the airfoil. These structures grow in size and convect downstream until the flow experiences a sudden and massive separation from the airfoil surface leading to the occurrence of so-called dynamic stall. A good understanding of the dynamics of the formation and growth of the leading-edge vortex system is essential for the efficient exploitation of lift augmentation and control of dynamic stall of the pitching airfoil. Past experimental studies on pitching airfoils have essentially been limited to the measurement of surface pressures only (e.g., Jumper, Schreck and Dimmick 1987, Acharya and Metawally 1990). There has been only one experiment (Shih *et al*) reported in the literature in which the velocity field around the pitching airfoil has been measured. There has been no study known to the authors in which both pressure and velocity data have been obtained. This paper presents the results of an ongoing experimental program on the study of the unsteady vortex dynamics of a two-dimensional pitching airfoil. Both velocity and pressure data are being obtained in these experiments.

EXPERIMENTAL PARTICULARS

The experiments are being performed in a specially constructed free-surface water channel. The airfoil being studied is a NACA 0015 profile of 35 cm chord (c) and 67 cm span. It is mounted with its span vertical inside the water channel. The experimental set-up is shown schematically in Fig.1. The airfoil is pitched at constant angular velocity ($\dot{\alpha}$) about its (spanwise) $c/4$-axis from an incidence (α) of 0 to about 30 degrees. Detailed data on surface pressure distribution along the chord and the velocity vector field around the airfoil on the suction side have been obtained as a function of the instantaneous angle of incidence. The pressure measurements were made using a finely spaced row of static pressure taps on the airfoil surface and a pressure transducer of adequate dynamic response. The instantaneous pressure data were processed to obtain phase-locked pressure distributions along the chord as a function of angle of incidence. The velocity vector field was obtained using the technique of particle-image velocimetry (PIV). For this purpose, the channel was seeded with micron size particles. The mid plane of the channel was illuminated by a laser light sheet, which was pulsed at an appropriate frequency. Employing computer controlled circuitry, multiple exposed particle photographs were obtained at a number of equal time intervals during the pitching motion. The particle images were processed using an image processor employing auto correlation techniques to obtain the instantaneous velocity vector field on the suction side of the airfoil. In order to achieve a high spatial resolution, the flow field was divided in to three regions, front, mid and aft, and the velocity field was measured in each of these regions separately. The results were later assembled together to obtain the composite flow field.

Pressure data have been obtained at several Reynolds numbers in the range $Re = U_\infty c/\nu \approx 50,000 - 220,000$, and at several pitching rates in the range $\alpha^+ = \dot{\alpha}c/U_\infty \approx 0.03-0.2$, where U_∞ is the freestream velocity and ν is the kinematic viscosity of water. Velocity measurements have been made at three different Reynolds numbers in the range 25,000 - 220,000 and at a nondimensional pitching rate α^+ of 0.072. The Reynolds numbers and pitch rate in two of these experiments were identical to those in which pressure data were obtained.

RESULTS

In the interest of brevity, only some typical results are shown and discussed here. More details will be presented at the conference. They will also reported in several forthcoming publications.

Figure 2 shows typical phase-locked pressure distributions at several instantaneous angles of incidence, measured at a Reynolds number of 5.2×10^4 and a nondimensional pitch rate of 0.072. The pressures are shown in terms of C_p defined in the usual way as

$$C_p = \frac{p - p_\infty}{\frac{1}{2}\rho U_\infty^2}$$

where p is the local surface pressure and p_∞ is the reference static pressure in the undisturbed free stream. The C_p distributions exhibit an initial leading-edge suction peak at about $0.01c$ from the nose. This peak grows rapidly with incidence till about 21 degrees. During this growth, the peak shifts towards the nose. After the initial growth, the suction peak suddenly collapses, while a secondary suction peak begins to form at $x/c \approx 0.2$. The secondary peak has a magnitude of about 3/4 of that of the first peak. This peak then slowly spreads out and moves downstream as the angle of attack increases further. The pressure distribution at very high angles of attack tends to approach the flat base pressure distribution of a bluff body wake.

The pressure data have been used to compute the unsteady lift coefficient C_l, defined, in the usual way, as the lift force per unit area of the airfoil surface normalized by the freestream dynamic head. The results for three different Reynolds numbers are shown in Fig.3. It is seen that there is no significant effect of Reynolds number on the lift except around the angle of maximum lift which is in the range of 26-30 degrees. The reduction in lift at larger incidences is due to the occurrence of dynamic stall. The second peak in the lift curves is most probably due to the effects of blockage, and should be ignored.

Figure 4(a) and 4(b)show the velocity vectors and the contours of spanwise vorticity ω_z in the front 1/3 region on the suction side of the airfoil at an incidence of 21 degrees. Only the front region is shown since at this incidence, nothing significant is occurring over the rest of the airfoil. The velocity vectors near the surface are almost parallel to the surface. Very high vorticity is seen next to the surface near the leading edge. This is due to the strong acceleration of the flow under the large favorable pressure gradient present in this region. The flow details at a slightly higher angle of incidence, namely 23 degrees are shown in Figs.4(c) and 4(d). Closed vorticity contours leaving the surface can be seen in this case. This indicates the formation of the leading-edge vortex. Note, however, that the strong vorticity contours still remain close to the surface. This causes the lift to continue to increase. Figure 4(e) shows the vorticity field over the entire suction side of the airfoil at an incidence of 26 degrees. The PIV data for the front, mid and aft sections of the airfoil are combined in this figure. There is some mismatch between the contours for the front and midsections. This is due to the fact that the results for these two sections correspond to two different realizations, which may not necessarily be identical, especially around the point of dynamic stall. The composite of the vector contours, however, clearly shows how the shear layer is lifting off the surface and is rolling to form the dynamic stall vortex. The lift reaches a maximum around this incidence. As the incidence increases, the dynamic stall vortex moves farther away from the wall and is rapidly convected downstream, leading to a reduction in the lift.

CONCLUSIONS

Pressure and velocity data have been obtained in the unsteady flow field around a pitching airfoil. Phase-locked surface pressure distributions exhibit a suction peak near the leading edge, whose magnitude increases up to an incidence of about 21-23 degrees depending on the Reynolds number. This increase is a result of the infusement of vorticity from the surface by the presence of the strong favorable pressure gradient. The peak collapses at higher angles as a secondary peak appears downstream. This peak is associated with the formation of the leading-edge vortex due to the accumulation of the vorticty in the region. The initial growth of vorticity and the subsequent formation of the vortex are all clearly seen from the vorticity information, obtained from the PIV measurements. The lift continues to increase so long as the vorticity remains close to the wall. Eventually, the vortex grows very large and is washed away from the surface, leading to a loss in lift. While these aspects of vortex dynamics leading to dynamic stall were all known qualitatively, the present experiments are the first to provide quantitative information on *both* surface pressure and velocity/vorticity on the pitching airfoil.

An examination of the pressure and lift data presented here shows that the present experiments in the water channel performed at relatively low Reynolds numbers seem to reproduce pressure and lift coefficients achieved at much higher Reynolds numbers in earlier wind tunnel experiments. This is presumably due to the higher freestream turbulence intensity in the water channel, which triggers early laminar-turbulent transition in the flow. This interesting (and practically significant) result will be discussed in some detail at the conference. Also more detailed data on the pressure and vorticity will be presented at that time.

ACKNOWLEDGMENTS

This work was supported by the United States Airforce Office of Scientific Research under Grant No. AFOSR-90-0131 with Capt. H. Helin and Maj. D. Fant as Program Managers. This support is gratefully acknowledged.

REFERENCES

ACHARYA, M. and Metwally, M.H. (1990) Evolution of the unsteady pressure field and vorticity production at the surface of a pitching airfoil. AIAA Paper No.90-1472.

JUMPER,E.J., SCHERECK, S.J. and DIMMICK, R.L. (1987) Lift-curve characteristics for an airfoil pitching at constant rate. J. Aircraft,24, 10, 680-687.

SHIH,C., LORENCO,L., VAN DOMMEIEN, L. and KROTHAPALLI, A. (1990) Unsteady flow past an airfoil pitched at constant rate. Proc. Int. Symposium on Nonsteady Fluid Dynamics, ASME FED, ed. J.A. Miller and D.P. Telionis, 92, 41-50.

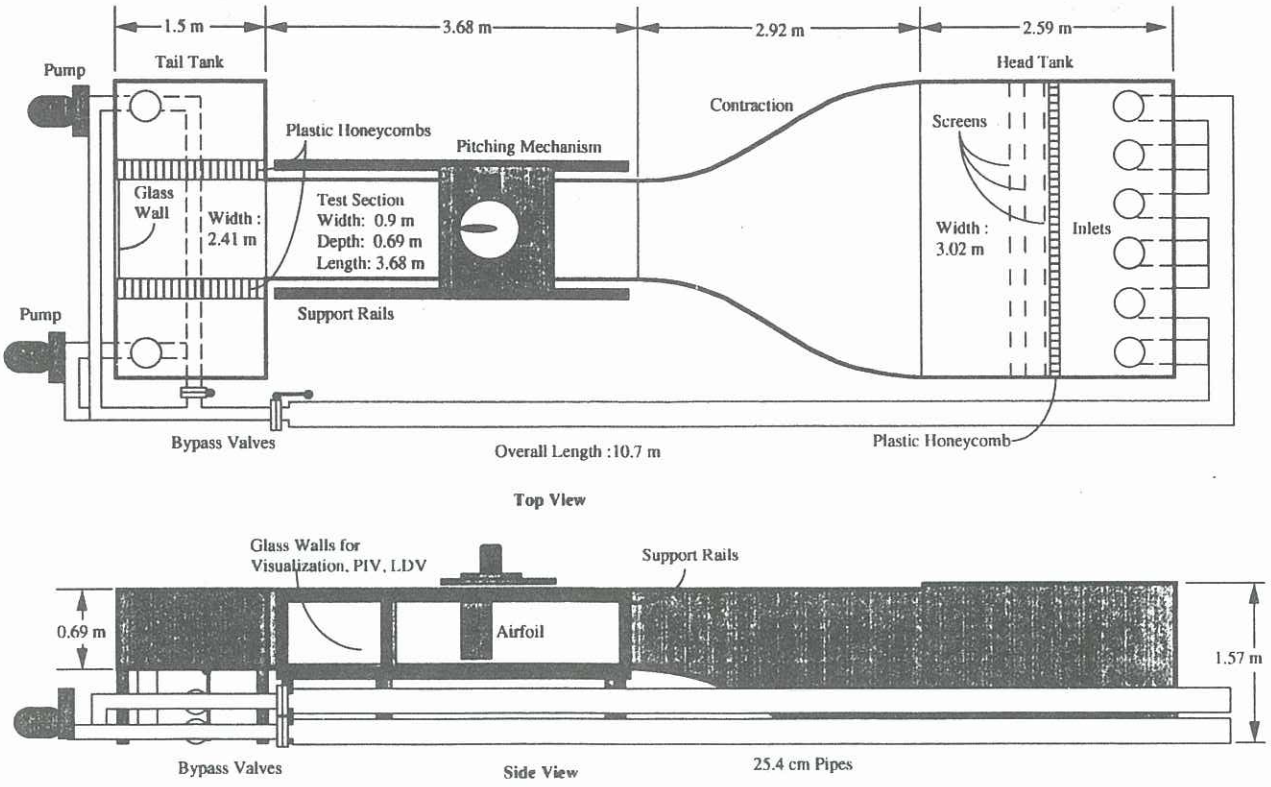

Figure 1. Schematic of the experimental set-up

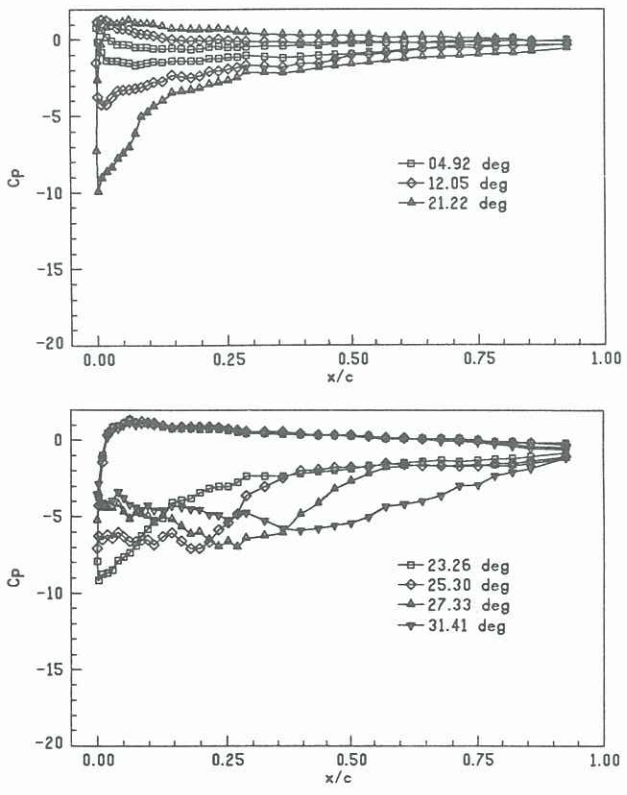

Figure 2. Typical pressure distributions along the airfoil surface at different incidences. $Re = 5.2{\times}10^4$; $\alpha^+ = 0.072$.

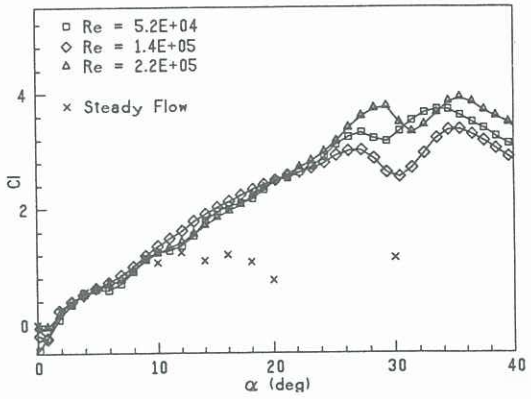

Figure 3. Variation of lift coefficient C_l with angle of incidence. $\alpha^+ = 0.072$.

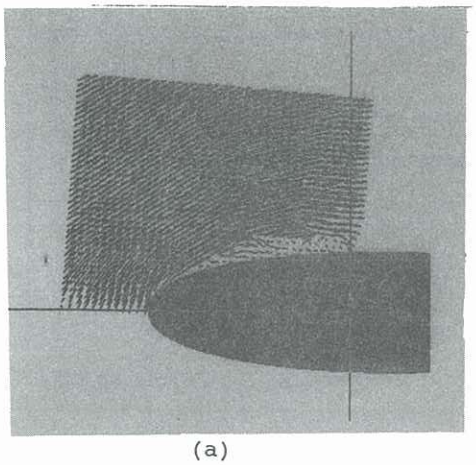

(a)

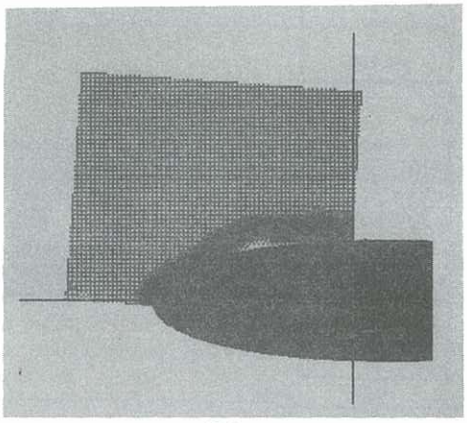

(b)

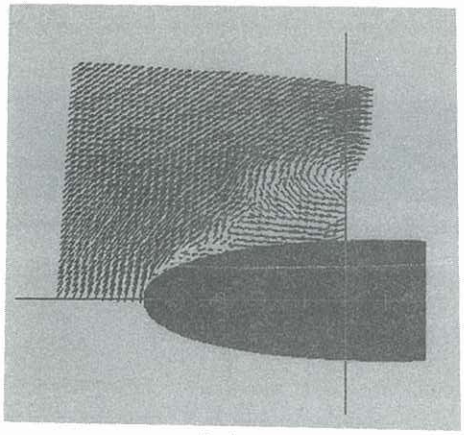

(c)

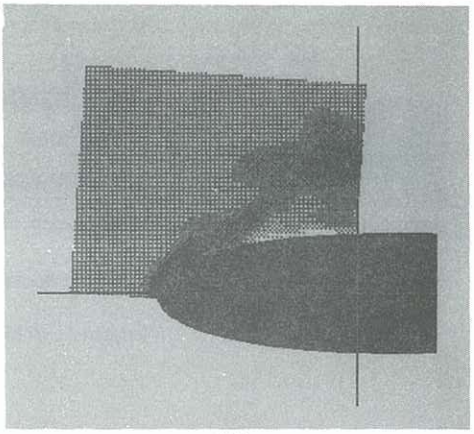

(d)

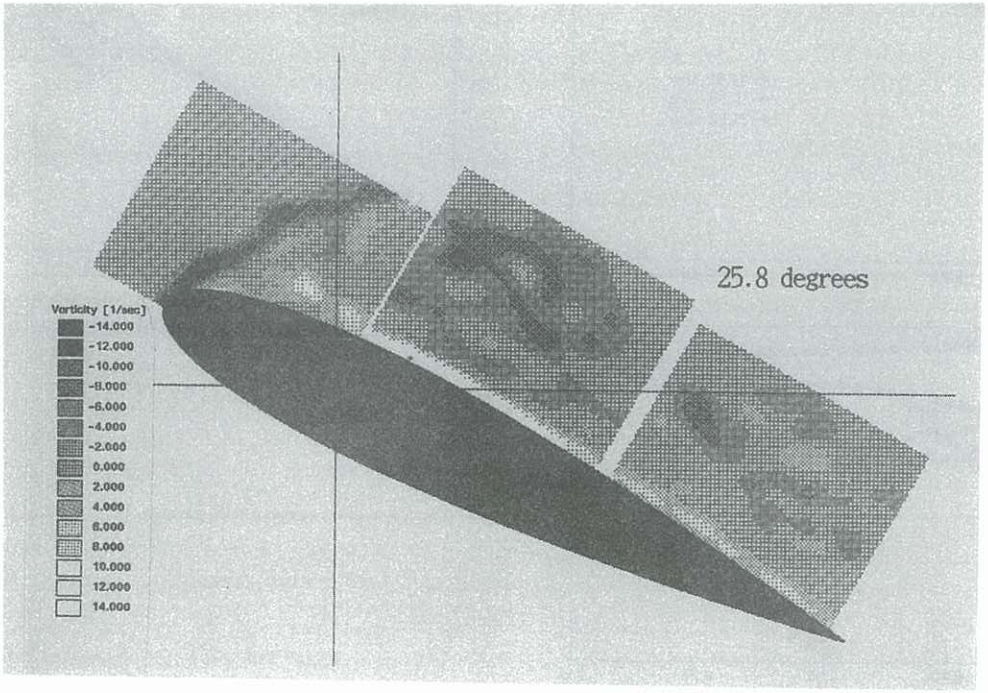

(e)

Figure 4. Typical velocity and vorticity results from PIV. (a), (b); Velocity vectors and contours of spanwise vorticity ω_z in the front 1/3 region of the airfoil at $\alpha = 21$ degrees. (c), (d); Velocity vectors and vorticity contours in the front region at $\alpha = 23$ degrees, (e) Vorticity contours at $\alpha = 26$ degrees over the entire airfoil.